

# Tunneling time and Faraday/Kerr effects in $\mathcal{PT}$ -symmetric systems

VLADIMIR GASPARIAN<sup>1</sup>, PENG GUO<sup>2,1,3</sup>, ANTONIO PÉREZ-GARRIDO<sup>4</sup> and ESTHER JÓDAR<sup>4</sup>

<sup>1</sup> Department of Physics and Engineering, California State University, Bakersfield, CA 93311, USA

<sup>2</sup> College of Arts and Sciences, Dakota State University, Madison, SD 57042, USA

<sup>3</sup> Kavli Institute for Theoretical Physics, University of California, Santa Barbara, CA 93106, USA

<sup>4</sup> Departamento de Física Aplicada. Hospital de Marina, Universidad Politécnica de Cartagena (UPCT), 30202 Cartagena, Murcia (Spain)

**Abstract** – We review the generalization of tunneling time and anomalous behaviour of Faraday and Kerr rotation angles in parity and time ( $\mathcal{PT}$ )-symmetric systems. Similarities of two phenomena are discussed, both exhibit a phase transition-like anomalous behaviour in certain range of model parameters. Anomalous behaviour of tunneling time and Faraday/Kerr angles in  $\mathcal{PT}$ -symmetric systems is caused by the motion of poles of scattering amplitudes in energy/frequency complex plane.

**Introduction.** – During the past two decades, parity-time ( $\mathcal{PT}$ )-symmetric Hamiltonians are studied in various areas of physics such as optics [1–3], quantum mechanics [4–6], and classical wave systems [7, 8]. For example, in optics,  $\mathcal{PT}$ -symmetric arrangements of gain and loss media have been studied, where the gain balances the loss, leading to interesting phenomena such as unidirectional invisibility and anomalous point oscillations [9, 10]. Note that although  $\mathcal{PT}$ -symmetric systems have been extensively studied and have theoretical and experimental support, their implementation in certain physical systems can still be difficult. Nevertheless, they remain an active research field with great potential for new discoveries and technical applications in optical isolators, sensors, magnetic storage, magneto-optical modulators, magneto-optical switches, and magneto-optical circulators.

In this letter, we present a brief review on (i) the generalization of the concept of tunneling time in  $\mathcal{PT}$  symmetric systems and (ii) some anomalous behaviours of magneto-optic effects in  $\mathcal{PT}$ -symmetric systems. Both quantum tunneling time and magneto-optic effects are the consequence of propagation of either quantum wave or optical wave through barriers, hence both phenomena are closely related to the transmission and reflection amplitudes of scattering of a quantum particle or light off barriers, and can be described in a similar framework.

In standard (Hermitian) quantum mechanics, both tunneling time of a quantum particle and Faraday and Kerr

rotations of a electromagnetic wave through real potential barriers are not new subjects, and a wide variety of theoretical and experimental work on both topics have been carried out extensively in the past:

(i) Tunneling time: Substantial research has been conducted on the tunneling time problem, see e.g. Refs. [11–13] and references therein). This area of exploration is particularly focused on nanostructures and mesoscopic systems with sizes smaller than 10nm. In such systems, the tunneling time assumes significance as it becomes a key factor in determining various transport properties. Notably, it plays a vital role in phenomena such as the frequency-dependent conductivity response of mesoscopic conductors [14] and the occurrence of adiabatic charge transport [15, 16]. More recently, another kind of problems have arisen in ultrafast science or in attosecond physics (e.g., the investigation of electron correlation effects, photoemission delay, ionization tunneling, etc), where tunneling time experiments play an important role as unique and powerful tool that allows in electronic monitoring with subatomic resolution both in space and time. The measurement of tunneling time in attosecond experiments (attosecond=10<sup>-18</sup>s) offers a fruitful opportunity to understand the role of time in quantum mechanics, which has been controversial since the appearance of quantum mechanics, see, e.g., Refs. [11, 13, 17].

(ii) Magneto-optic effects: The development of electromagnetic theory and atomic physics has been largely influ-

enced by the study of the magneto-optic effects as Faraday rotation (FR) and Kerr rotation (KR). In these magneto-optical phenomena, an electromagnetic wave propagates through a medium altered by the presence of an external magnetic field. In such magneto-optical materials (also referred as gyrotropic or gyromagnetic), left- and right-rotating elliptical polarizations propagating at different speeds result in a rotation of the planes of the transmitted (FR) and reflected (KR) light. FR and KR effects are essential for optical communication technologies [18], optical amplifiers [3, 19], and photonic crystals [20, 21]. In addition, the KR is also an extremely accurate and versatile research tool and can be used to determine quantities, such as anisotropy constants, exchange-coupling strengths and Curie temperatures (see, e.g. [22]).

**General theory of tunneling time and magneto-optic effects in  $\mathcal{PT}$ -symmetric systems.** – A brief summary of general theory of tunneling time and magneto-optic effects in  $\mathcal{PT}$ -symmetric systems is given in this section, more details can be found in [23–26].

*Tunneling time.* The concept of tunneling or delay time for a quantum particle tunneling through real potential barriers is conventionally defined through the integrated density of states, which is proportional to the imaginary part of full Green's function of systems and positive definite in a real potential scattering theory. Following the definition in Refs. [27–29], two components of the traversal time  $\tau_E$  can be introduced by ( $\hbar = 1$ )

$$\tau_E = \tau_2 + i\tau_1 = - \int_{-\frac{\Lambda}{2}}^{\frac{\Lambda}{2}} dx \langle x | \hat{G}(E) | x \rangle, \quad (1)$$

where  $\tau_1$  and  $\tau_2$  represent Büttiker-Landauer tunneling time and the Landauer resistance respectively. The  $\Lambda$  stands for the length of potential barrier, and the  $\hat{G}(E) = \frac{1}{E - \hat{H}}$  is the Green's function operator of system. As shown in Refs. [28, 29], two components of the traversal time  $\tau_E$  are linked to the scattering and transport amplitudes explicitly by

$$\tau_2 + i\tau_1 = \frac{d \ln [t(k)]}{dE} + \frac{r^{(l)}(k) + r^{(r)}(k)}{4E}, \quad (2)$$

where  $t(k)$  and  $r^{(l/r)}(k)$  are the transmission and left/right reflection amplitudes respectively, and  $k = \sqrt{2mE}$  is the momentum of particle. The transmission and reflection amplitudes can be obtained by finding scattering solutions of Schrödinger equation,

$$\hat{H}|\Psi_E\rangle = E|\Psi_E\rangle, \quad \hat{H} = -\frac{1}{2m} \frac{d^2}{dx^2} + V(x), \quad (3)$$

where  $m$  denotes the mass of particle, and  $V(x)$  is the interaction potential.

In the conventional real potential scattering theory, the development of concept of tunneling or delay time is fundamentally based on counting the probability that a particle spends inside of a barrier, see e.g. Refs. [30–32]. However, in complex potential scattering theory, the norm of

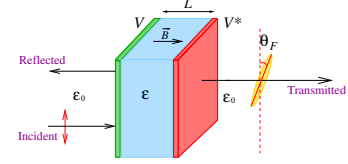


Fig. 1: Demo plot of a  $\mathcal{PT}$ -symmetric dielectric slab model with two balanced complex narrow slabs placed at both ends of a real dielectric slab.

states is no longer conserved, the probability interpretation of tunneling time becomes problematic. This can be understood by examining the spectral representation of Green's function in a complex potential scattering theory, which now depends on the eigenstates of both  $\hat{H}$  and its adjoint  $\hat{H}^\dagger$ ,

$$\hat{G}(E) = \sum_i \frac{|\Psi_{E_i}\rangle \langle \tilde{\Psi}_{E_i}|}{E - E_i}, \quad (4)$$

where

$$\hat{H}^\dagger |\tilde{\Psi}_E\rangle = E |\tilde{\Psi}_E\rangle. \quad (5)$$

Hence, the discontinuity of Green's function crossing the branch cut in complex  $E$ -plane is in general a complex function, and it is no longer equivalent to the imaginary part of Green's function, see Ref. [23]. As shown in Ref. [23], under the constraints of  $\mathcal{PT}$  symmetry, the discontinuity of Green's function is fortunately still a real function and identical to imaginary part of Green's function. However, as the consequence of norm violation with a complex potential, positivity of the imaginary part of Green's function is not guaranteed. Its relevance to the conventional definition of density of states is hence lost. Now one is facing the challenge of how the concept of tunneling time should be generalized and defined properly.

In this review letter, the tunneling time through  $\mathcal{PT}$ -symmetric barriers is still defined by Eq. (1). The imaginary part of Green's function is now referred as generalized density of states of a  $\mathcal{PT}$ -symmetric system. In a  $\mathcal{PT}$ -symmetric system,  $\tau_1$  now may be interpreted as generalized concept of Büttiker-Landauer tunneling time. The positivity and negativity of generalized tunneling time  $\tau_1$  simply reflects the nature of potential barriers that either tend to keep a particle in or force it out. The negative value portion of  $\tau_1$  is thus physically inaccessible and hence behave similar to a forbidden gap in a periodic system.

*Magneto-optic effects.* We consider an incident linearly polarized electromagnetic plane wave with an angular frequency  $\omega$  entering the system from the left, propagating along the  $x$  direction. The electric field's polarization direction of the incident wave is aligned with the  $z$ -axis:  $\mathbf{E}_0(x) = e^{i\frac{\omega}{c}\sqrt{\epsilon_0}x} \hat{z}$ , where  $\epsilon_0$  denotes the dielectric constant of vacuum. A magnetic field  $\mathbf{B}$  is applied in the  $x$ -direction, as depicted in Fig. 1. The scattering of EM

wave is described by, see e.g. Refs. [33, 34],

$$\left[ \frac{d^2}{dx^2} + \frac{\omega^2 \epsilon_{\pm}(x)}{c^2} \right] E_{\pm}(x) = 0, \quad (6)$$

where  $E_{\pm} = E_y \pm iE_z$  represents the circularly polarized electric fields. The variable  $\epsilon_{\pm}(x)$  is defined as follows:

$$\epsilon_{\pm}(x) = \begin{cases} \epsilon + V(x) \pm g, & \text{if } x \in [-\frac{L}{2}, \frac{L}{2}], \\ \epsilon_0, & \text{otherwise,} \end{cases} \quad (7)$$

where  $L$  represents the length of dielectric slab and  $\epsilon$  is positive and real permittivity of the slab, see Fig. 1. The  $V(x)$  denotes the additional potential barriers that are placed inside of the slab, which can be easily manipulated and adjusted to implement  $\mathcal{PT}$  symmetry requirement. The  $g$  is the gyrotropic vector along the magnetic-field direction. The external magnetic field  $\mathbf{B}$  is included into the gyrotropic vector  $g$  to make the calculations valid for the cases of both external magnetic fields and magneto-optic materials. The magnetic field causes the direction of linear polarization of both transmitted and reflected wave to rotate. As a consequence, both the outgoing transmitted and reflected waves exhibits elliptical polarization. The major axis of the ellipse is rotated relative to the original polarization direction. The real part of the rotation angle describes the change in polarization for linearly polarized light, while the imaginary part indicates the ellipticity of the transmitted or reflected light.

The complex rotational parameters characterizing the transmitted light can be expressed in terms of transmission amplitudes by

$$\theta_2^T + i\theta_1^T = \frac{1}{2} \ln \frac{t_+(\omega)}{t_-(\omega)}, \quad (8)$$

where  $t_{\pm}$  represent the transmission amplitudes of transmitted electric fields. In the case of a weak magnetic field ( $g \ll 1$ ), a perturbation expansion can be applied. The leading-order contribution can be obtained by expanding  $t_{\pm}$  around the refractive index of the slab in the absence of the magnetic field  $\mathbf{B}$ :

$$\theta_2^T + i\theta_1^T = \frac{g}{2n} \frac{\partial \ln [t(\omega)]}{\partial n}, \quad (9)$$

where,  $n = \sqrt{\epsilon}$  represents the refractive index of the slab. Similarly, the leading-order expressions of complex angles of Kerr rotation, in the case of a weak magnetic field, are given by:

$$\theta_2^{R(l/r)} + i\theta_1^{R(l/r)} = \frac{g}{2n} \frac{\partial \ln [r^{(l/r)}(\omega)]}{\partial n}, \quad (10)$$

where  $r^{(l/r)}$  is the left/right reflection amplitudes in the absence of magnetic field  $\mathbf{B}$ .

**$\mathcal{PT}$  symmetry constraints on scattering amplitudes.** The  $\mathcal{PT}$  symmetry can be implemented in quantum tunneling time and magneto-optic effects by imposing conditions on interaction potential in Schrödinger equation and

on dielectric permittivity in Eq.(6):  $V(x) = V^*(-x)$ . As discussed in Ref. [23], the parametrization of scattering matrix only requires three independent real functions in a  $\mathcal{PT}$ -symmetric system: one inelasticity,  $\eta \in [1, \infty]$ , and two phaseshifts,  $\delta_{1,2}$ . In terms of  $\eta$  and  $\delta_{1,2}$ , the transmission and reflection amplitudes are given by

$$t = \eta \frac{e^{2i\delta_1} + e^{2i\delta_2}}{2},$$

$$r^{(r/l)} = \eta \frac{e^{2i\delta_1} - e^{2i\delta_2}}{2} \pm i\sqrt{\eta^2 - 1} e^{i(\delta_1 + \delta_2)}. \quad (11)$$

As the consequence of  $\mathcal{PT}$  symmetry constraints, two components of the traversal time are also given in terms of  $\eta$  and  $\delta_{1,2}$  by

$$\tau_1 = \frac{d(\delta_1 + \delta_2)}{dE} + \eta \frac{\sin(2\delta_1) - \sin(2\delta_2)}{4E},$$

$$\tau_2 = \frac{d \ln [\eta \cos(\delta_1 - \delta_2)]}{dE} + \eta \frac{\cos^2 \delta_1 - \cos^2 \delta_2}{2E}. \quad (12)$$

Only three FR and KR angles are independent, the FR and KR angles are given in terms of  $\eta$  and  $\delta_{1,2}$  by

$$\theta_1^T = \theta_1^R = \frac{g}{2n} \frac{\partial(\delta_1 + \delta_2)}{\partial n}, \quad \theta_2^T = \frac{g}{2n} \frac{\partial \ln [\eta \cos(\delta_1 - \delta_2)]}{\partial n},$$

$$\theta_2^{R(r/l)} = \frac{g}{2n} \frac{\partial}{\partial n} \ln \left| \eta \sin(\delta_1 - \delta_2) \pm \sqrt{\eta^2 - 1} \right|. \quad (13)$$

$\theta_2^{R(r/l)}$  and  $\theta_2^T$  are related by  $\theta_2^{R(r)} + \theta_2^{R(l)} = \frac{2T}{T-1} \theta_2^T$ , where  $T = \eta^2 \cos^2(\delta_1 - \delta_2)$  denotes the transmission coefficient.

#### A simple exact solvable $\mathcal{PT}$ -symmetric model. –

A simple  $\mathcal{PT}$ -symmetric contact interaction potential model is adopted in this letter to illustrate some usual features in both tunneling time and magneto-optic effects in  $\mathcal{PT}$ -symmetric systems. The  $\mathcal{PT}$ -symmetric interaction potential for a single cell of barrier is chosen as

$$V(x) = V\delta(x + \frac{L}{2}) + V^*\delta(x - \frac{L}{2}), \quad V = |V|e^{i\varphi_V} = V_1 + iV_2, \quad (14)$$

which represents two complex-conjugate impurities placed inside of a single cell. One is absorbing with loss and another is emissive with an equal amount of gain. The closed forms of scattering solutions can be obtained for contact interaction potential model:

(i) Transmission and reflection amplitudes for a quantum particle tunneling through a single cell of barrier of length  $\Lambda$  ( $\Lambda = L + L_0$ ) are given by

$$t_0(k) = \frac{\csc(kL)e^{ikL_0}}{\mathcal{R}(k) - i\mathcal{I}(k)}, \quad r_0^{(l/r)}(k) = i \frac{Q^{(l/r)}(k)e^{ikL_0}}{\mathcal{R}(k) - i\mathcal{I}(k)}, \quad (15)$$

where  $L_0$  stands for the separation between two slabs, and

$$\mathcal{R}(k) = \cot(kL) + 2 \frac{m|V| \cos \varphi_V}{k},$$

$$\mathcal{I}(k) = 1 - 2 \left( \frac{m|V|}{k} \right)^2 - 2 \left( \frac{m|V| \cos \varphi_V}{k} \right) \cot(kL),$$

$$Q^{(l/r)}(k) = -2 \frac{m|V|}{k} \left[ \frac{\cos(kL \mp \varphi_V)}{\sin(kL)} + \frac{m|V|}{k} \right]. \quad (16)$$

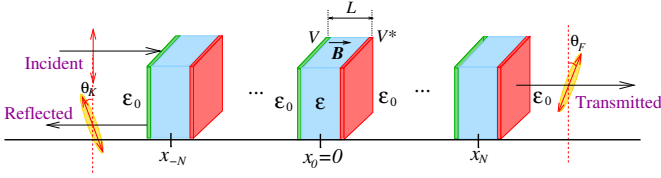


Fig. 2: Schematic of a one-dimensional multiple cells  $\mathcal{PT}$ -symmetric photonic heterostructure.

(ii) The transmission and reflection amplitudes in Eq. (15) also apply in the case of Faraday and Kerr effects for a single cell with slab of length  $\Lambda$  by replacing  $k$  by  $\frac{\omega_n}{c}$ . The expression of functions  $\mathcal{R}(\omega)$ ,  $\mathcal{I}(\omega)$  and  $Q^{(r/l)}(\omega)$  are given in Eq.(15) and Eq.(18) in Ref. [26].

*Periodic multiple cells  $\mathcal{PT}$ -symmetric systems.* It is known that when the wave propagation through a medium is described by a differential equation of second order, the expression for the total transmission from the finite periodic system for any waves (sound and electromagnetic) depends on the unit cell transmission, the Bloch phase and the total number of cells. The infinite periodic  $\mathcal{PT}$ -symmetric structures exhibit unusual properties, including the band structure, Bloch oscillations, unidirectional propagation and enhanced sensitivity, see e.g., Refs. [35–38] and Refs. therein. However, the case of scattering in a finite periodic system composed of an arbitrary number of cells/scatters has been less investigated, despite that any open quantum system generally consists of a finite system coupled with an infinite environment. In Hermitian theory, the averaged physical observables of a finite system approach the limit that depends on the crystal-momentum of an infinite periodic system as the size of a finite system is increased. However in  $\mathcal{PT}$ -symmetric systems, new challenges emerge, the large size limit of a finite size system is only well-defined conditionally.

The  $\mathcal{PT}$ -periodic symmetric structure that consists of  $2N + 1$  cells, see Fig.2, can be assembled on top of single cell. Following Refs. [25, 26, 39], a generic expressions for the transmission and reflection amplitudes for  $2N + 1$  cells of  $\mathcal{PT}$ -periodic symmetric structure in both tunneling time and magneto-optic effects cases can be presented as:

$$t = \frac{1}{\cos(\beta(2N+1)\Lambda) + iIm\left[\frac{1}{t_0}\right] \frac{\sin(\beta(2N+1)\Lambda)}{\sin(\beta\Lambda)}},$$

$$\frac{r^{(l/r)}}{t} = \frac{r_0^{(l/r)}}{t_0} \frac{\sin(\beta(2N+1)\Lambda)}{\sin(\beta\Lambda)}. \quad (17)$$

The  $\beta$  plays the role of crystal-momentum for a periodic lattice and is related to  $k$  or  $\omega$  by

$$\cos(\beta\Lambda) = Re\left[\frac{1}{t_0}\right]. \quad (18)$$

The factor  $\frac{\sin(\beta(2N+1)\Lambda)}{\sin(\beta\Lambda)}$  in both transmission and reflection amplitudes reflects the combined interference and

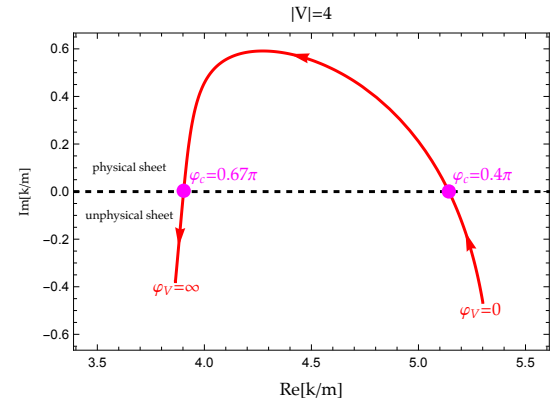


Fig. 3: The motion of poles in complex  $k/m$ -plane as a function of increasing  $\varphi_V$  for tunneling time of a single cell defined in Eq.(15) and Eq.(16). The arrows indicate increasing  $\varphi_V$  directions. The  $\varphi_V$  values of spectral singularities are indicated by  $\varphi_c$ 's. The model parameters are taken as:  $|V| = 4$  and  $mL = 1$ .

diffraction effects in finite periodic systems, which occur naturally in Hermitian one-dimensional finite size periodic systems. It is interesting to see that Eq.(17) hold up for both Hermitian and  $\mathcal{PT}$ -symmetric systems, which is highly non-trivial since the usual probability conservation property for Hermitian systems must be generalized in  $\mathcal{PT}$ -symmetric systems. As pointed out in Ref. [25], the scattering amplitudes for a periodic multiple cells system can be related to single cell amplitudes in a compact fashion. This is ultimately due to the factorization of dynamics living in two distinct physical scales: short-range dynamics in a single cell and long-range collective effects of the periodic structure of entire system. The short-range interaction dynamics is described by single cell scattering amplitudes and the  $\beta$  represents the long range correlation effect of entire lattice system. The occurrence of factorization of short-range dynamics and long-range collective mode has been known in both condensed matter physics and nuclear/hadron physics. As examples, particles interacting with short-range potential in a periodic box or trap, quantization conditions can be given in a compact formula that is known as Korringa–Kohn–Rostoker method [40, 41] in condensed matter physics, Lüscher formula [42] in lattice quantum chromodynamics and Busch-Englert–Rzażewski–Wilkens formula [43] in nuclear physics community. Other related useful discussions can be found in e.g. Refs. [44–48].

*Spectral singularities and their impact on tunneling time and magneto-optic effects in  $\mathcal{PT}$ -symmetric systems.* Two types of singularities are present in scattering amplitudes: (1) a branch cut sitting along the positive real axis in complex  $k$  or  $\omega$ -plane that separate physical sheet (the first Riemann sheet) and unphysical sheet (the second Riemann sheet); (2) poles of transmission and reflection

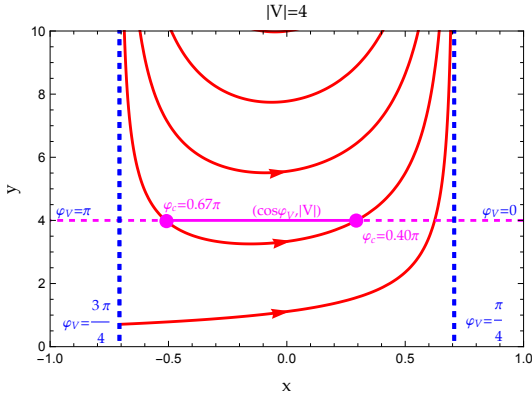


Fig. 4: Spectral singularities condition plot: the parametric plot of solid red curve is generated with  $(x, y)$  coordinates given by left-hand side of Eq.(21) as the function of  $k/m$ . The solid red curve is bound by two blue vertical lines located at  $x = \pm \frac{1}{\sqrt{2}}$ . The purple line is generated with coordinates of  $(\cos \varphi_V, |V|)$  by varying  $\varphi_V$  in the range of  $[0, \pi]$ . The arrows indicate increasing  $k/m$  directions. The spectral singularities for fixed  $m|V|$  are given by intersection of purple line and red curve. The model parameters are chosen as:  $|V| = 4$ , and  $mL = 1$ .

amplitudes. These poles are called spectral singularities of a non-Hermitian Hamiltonian when they show up on real axis [49–51], which yields divergences of reflection and transmission coefficients of scattered states.

The motion of poles in complex  $k$  or  $\omega$ -plane, Fig. 3, has some profound impact on the value of  $\tau_1$  in tunneling time and Faraday and Kerr rotation angles  $\theta_1^T$  and  $\theta_1^R$  in  $\mathcal{PT}$ -symmetric systems. The location of these poles are model parameters dependent and can be found by solving  $1/t = 0$ . The normal or anomalous behaviours of  $\tau_1$  and  $\theta_1^{T/R}$  are determined by the location of poles: when the poles are all located in unphysical sheet (the second Riemann sheet),  $\tau_1$  and  $\theta_1^{T/R}$  remains positive. As poles moves close to and ultimately cross real axis into physical sheet (the first Riemann sheet), the poles generate a enhancement in  $\tau_1$  and  $\theta_1^{T/R}$  near the location of poles. The spectral singularities occur when poles are located on real axis, the transmission and reflection amplitudes diverge at location of poles. This can be easily understood with the motion of a single pole. Near the pole, the transmission amplitude is approximated by

$$t(k) \propto \frac{1}{k - k_{pole}} = \frac{k - k_{re} - i\gamma}{(k - k_{re})^2 + \gamma^2}, \quad (19)$$

where  $k_{pole} = k_{re} + i\gamma$ , being  $k_{re}$  and  $\gamma$  the real and imaginary parts of pole position. The location of pole in physical sheet or unphysical sheet is determined by sign of  $\gamma$ : unphysical sheet if  $\gamma < 0$  and physical sheet if  $\gamma > 0$ . The tunneling time  $\tau_1$  or Faraday/Kerr rotation angle  $\theta_1^{T/R}$

near the pole is thus dominated by

$$\tau_1 \sim \frac{m}{k} \frac{\gamma}{(k - k_{re})^2 + \gamma^2}, \quad (20)$$

hence as pole moves across real axis into physical sheet,  $\gamma$  changes its sign.

The location of moving poles are controlled by model parameters. The spectral singularities only occur in certain range of model parameters, the boundary of the range of model parameters hence separate normal behaviour of tunneling time and Faraday/Kerr rotation angles where  $\tau_1$  and  $\theta_1^{T/R}$  always remain positive from anomalous behaviours where  $\tau_1$  and  $\theta_1^{T/R}$  may turn negative near location of spectral singularities. When the model parameters are varied continuously, the tunneling time and Faraday/Kerr rotation angles in  $\mathcal{PT}$ -symmetric systems hence experience a phase transition-like transformation. Using expressions in Eq.(15) and Eq.(16) as a simple example, the conditions for spectral singularities are given by considering  $1/t_0(k) = 0$ :

$$\left( -\frac{\cot(kL) |\sin(kL)|}{\sqrt{2}}, \frac{k/m}{\sqrt{2} |\sin(kL)|} \right) = (\cos \varphi_V, |V|). \quad (21)$$

The solutions of spectral singularities can be visualized graphically by observing the intersection of a curve and a line with  $(x, y)$  coordinates given by both sides of Eq.(21) for a fixed  $|V|$ , see Fig. 4 as a example. For a fixed  $|V| = 4$ , the solutions of spectral singularities can only be found in a finite range:  $\varphi_V \in [0.4\pi, 0.67\pi]$ , in which the poles appear in physical sheet, anomalous behaviour of tunneling time and Faraday/Kerr rotation angles occur and  $\tau_1$  and  $\theta_1^{T/R}$  may turn negative. For a fixed  $|V| = 4$ , only a single pole solution can be found in complex  $k$ -plane, the motion of pole as  $\varphi_V$  is increased is illustrated in Fig.3.

For a large  $N$  system, the situation is even more interesting, the band structure and EPs start getting involved, competing with poles and playing the roles in turning  $\tau_1$  and  $\theta_1^{T/R}$ , see detailed discussion in Ref. [25]. The band structure of system is clearly visible for even small size systems. The number of poles grow drastically with size, and the distribution of poles split into bands. When the poles show up inside an allowed band of system and all move across the real axis, they tend to flip the sign of entire band. In some bands where two bands start merging together at exceptional point, the exceptional points tend to force  $\tau_1$  and  $\theta_1^{T/R}$  approaching zero and starts to competing with poles, so the  $\mathcal{PT}$ -symmetric systems become almost transparent near EPs. The fate of  $\tau_1$  and  $\theta_1^{T/R}$  near EPs now is the result of two competing forces: the poles and EPs.

*Large  $N$  limit.* As number of cells is increased, all traversal time  $\tau_{1,2}$  and FR and KR angles demonstrate fast oscillating behaviour due to  $\sin(\beta(2N + 1)\Lambda)$  and  $\cos(\beta(2N + 1)\Lambda)$  functions in transmission and reflection amplitudes. For the large  $N$  systems, we can introduce

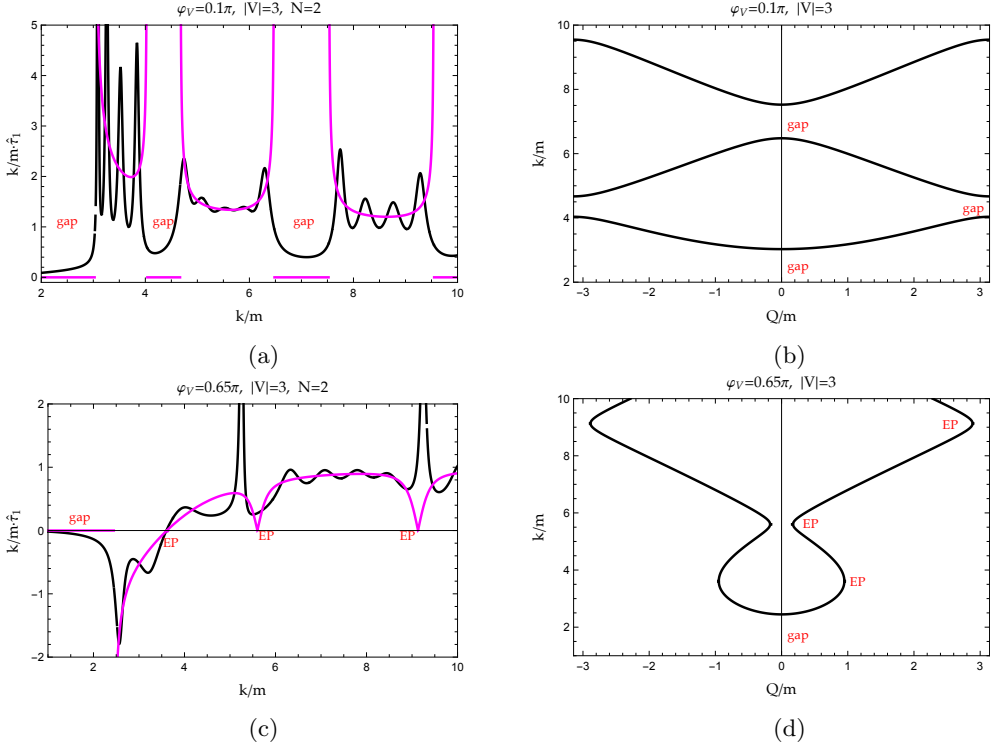


Fig. 5: (a & c) Comparison of  $\frac{k}{m}\hat{\tau}_1$  (solid black) together with  $\frac{k}{m}\frac{dRe[Q]}{dE}$  (solid purple/light grey) in unbroken and broken  $\mathcal{PT}$ -symmetric phase; (b & d) The corresponding band structure plot in unbroken and broken  $\mathcal{PT}$ -symmetric phase. The rest of parameters are taken as:  $mL = 1$  and  $ma = 0.2$ , where  $|V|$  is dimensionless.

the traversal time per unit cell and FR and KR angles per unit cell, such as

$$\hat{\tau}_{1,2} = \frac{\tau_{1,2}}{(2N+1)\Lambda}. \quad (22)$$

The  $N \rightarrow \infty$  limit may be approached by adding a small imaginary part to  $\beta$ :  $\beta \rightarrow \beta + i\epsilon$ , where  $\epsilon \gg \frac{1}{(2N+1)\Lambda}$ . As discussed in Ref. [25], adding a small imaginary part to  $\beta$  is justified by considering the averaged FR and KR angles per unit cell, which ultimately smooth out the fast oscillating behaviour of  $\tau_{1,2}$  and FR and KR angles. Therefore, as  $N \rightarrow \infty$ , the two components of traversal time per unit cell approach

$$\hat{\tau}_1 - i\hat{\tau}_2 \xrightarrow{N \rightarrow \infty} \frac{d\beta}{dE}, \quad (23)$$

and FR and KR angles per unit cell approach

$$\hat{\theta}_1^T - i\hat{\theta}_2^T \xrightarrow{N \rightarrow \infty} \frac{g}{2n} \frac{\partial \beta}{\partial n}, \quad \hat{\theta}_2^{R(r/l)} \xrightarrow{N \rightarrow \infty} 0. \quad (24)$$

The examples of tunneling time per unit cell for a  $\mathcal{PT}$ -symmetric finite system with five cells are shown in Fig. 5, compared with the large  $N$  limit results. As we can see in Fig. 5, the  $\tau_1$  oscillate around the large  $N$  limit results. Even for the small size system, we can see clearly that the band structure of infinite periodic system is already showing up. In broken  $\mathcal{PT}$ -symmetric phase in Fig. 5, EPs can be visualized even for a small size system, where two

neighbouring bands merge and the  $\mathcal{PT}$  becomes totally transparent:  $\tau_1$  approach zero. FR/KR angles show the similar behaviour, see e.g. Fig. 4 and Fig. 5 in Ref. [26].

The limiting cases in Eq.(23) and Eq.(24) work well and are mathematically well-defined in bands where spectral singularities are absent on real axis, the poles are all either in physical sheet or already all crossed real axis into unphysical sheet. The large  $N$  limit is well defined and can be achieved by either averaging fast oscillating behaviour of  $\tau_E$  or using  $i\epsilon$ -prescription by shifting  $k$  off real axis into complex plane. However, in the bands where the divergent singularities show up on the real axis and the band is still in the middle of transition between all positive and all negative band of  $\tau_1$  and  $\theta_1^{T/R}$ , see e.g. Fig. 8 in Ref. [25], Eq.(23) and Eq.(24) break down, and large  $N$  limit becomes ambiguous and problematic. The question of how to define a physically meaningful large  $N$  limit in presence of spectral singularities is still open.

**Summary.** — We give a brief review on recent development of the generalization of tunneling time and anomalous behaviour of Faraday and Kerr rotation angles in  $\mathcal{PT}$ -symmetric systems. Both phenomena are closely related to each other, associated with a generalized density of states and exhibit a phase transition-like anomalous behaviour in certain range of model parameters. Anomalous behaviour of tunneling time and Faraday/Kerr angles in  $\mathcal{PT}$ -symmetric systems is directly related to the motion of

poles of scattering amplitudes in energy/frequency complex plane. When poles show up in physical sheets, the value of tunneling time  $\tau_1$  and Faraday and Kerr rotation angles  $\theta_1^{T/R}$  may turn negative, which may be considered as anomalous phase of  $\mathcal{PT}$ -symmetric systems. On the contrary, when all poles remain in unphysical sheet, tunneling time and Faraday/Kerr angles of  $\mathcal{PT}$ -symmetric systems behave just as normal Hermitian systems, which may be considered as normal phase of systems. Both  $\tau_1$  and  $\theta_1^{T/R}$  exhibit a strong enhancement when the poles move close to real axis where spectral singularities occur.

**Acknowledgement .** – V.G., A.P-G. and E.J. would like to thank UPCT for partial financial support through "Maria Zambrano ayudas para la recualificación del sistema universitario español 2021-2023" financed by Spanish Ministry of Universities with funds "Next Generation" of EU. This research was supported in part by the National Science Foundation under Grant No. NSF PHY-1748958.

## REFERENCES

- [1] YOSHINO T., *Journal of the Optical Society of America B Optical Physics*, **22** (2005) 1856.
- [2] ZAMANI M., GHANAATSHOAR M. and ALISAFEE H., *Journal of the Optical Society of America B Optical Physics*, **28** (2011) 2637.
- [3] CORZO N. V., MARINO A. M., JONES K. M. and LETT P. D., *Phys. Rev. Lett.*, **109** (2012) 043602.
- [4] RAZAVY M. and MUGA J. G., *Physics Today*, **57** (2004) 66.
- [5] MOSTAFAZADEH A., *Journal of Mathematical Physics*, **43** (2002) 2814.
- [6] GARMON S., GIANFREDA M. and HATANO N., *Phys. Rev. A*, **92** (2015) 022125.
- [7] MERKEL A., ROMERO-GARCÍA V., GROBY J.-P., LI J. and CHRISTENSEN J., *Phys. Rev. B*, **98** (2018) 201102.
- [8] ZHU X., RAMEZANI H., SHI C., ZHU J. and ZHANG X., *Physical Review X*, **4** (2014) 031042.
- [9] LIN Z., RAMEZANI H., EICHELKRAUT T., KOTTOS T., CAO H. and CHRISTODOULIDES D. N., *Phys. Rev. Lett.*, **106** (2011) 213901.
- [10] FENG L., XU Y.-L., FEGADOLLI W. S., LU M.-H., OLIVEIRA J. E. B., ALMEIDA V. R., CHEN Y.-F. and SCHERER A., *Nature Materials*, **12** (2013) 108.
- [11] LANDAUER R. and MARTIN T., *Rev. Mod. Phys.*, **66** (1994) 217.
- [12] FAYER M. and FAYER P., *Elements of Quantum Mechanics* (Oxford University Press) 2001.
- [13] GASPARIAN V., ORTUÑO M., SCHÖN G. and SIMON U., in *Handbook of nanostructured materials and nanotechnology* (Academic Press, San Diego) 2000.
- [14] BÜTTIKER M., THOMAS H. and PRÊTRE A., *Zeitschrift fur Physik B Condensed Matter*, **94** (1994) 133.
- [15] BROUWER P. W., *Phys. Rev. B*, **58** (1998) R10135.
- [16] ZHOU F., SPIVAK B. and ALTSHULER B., *Phys. Rev. Lett.*, **82** (1999) 608.
- [17] MUGA J., PALAO J., NAVARRO B. and EGUSQUIZA I., *Physics Reports*, **395** (2004) 357.
- [18] BIRCH K. P., *Optics Communications*, **43** (1982) 79.
- [19] STUBKJAER K. E., *IEEE Journal of Selected Topics in Quantum Electronics*, **6** (2000) 1428.
- [20] WANG Z., CHONG Y. D., JOANNOPOULOS J. D. and SOLJAČIĆ M., *Phys. Rev. Lett.*, **100** (2008) 013905.
- [21] WANG Z., CHONG Y., JOANNOPOULOS J. D. and SOLJAČIĆ M., *Nature*, **461** (2009) 772.
- [22] MCGEE N. W. E., JOHNSON M. T., DE VRIES J. J. and AAN DE STEGGE J., *Journal of Applied Physics*, **73** (1993) 3418.
- [23] GUO P. and GASPARIAN V., *Phys. Rev. Research*, **4** (2022) 023083.
- [24] GASPARIAN V., GUO P. and JÓDAR E., *Phys. Lett. A*, **453** (2022) 128473.
- [25] GUO P., GASPARIAN V., JÓDAR E. and WISEHART C., *Phys. Rev. A*, **107** (2023) 032210.
- [26] PEREZ-GARRIDO A., GUO P., GASPARIAN V. and JÓDAR E., *Phys. Rev. A*, **107** (2023) 053504.
- [27] GASPARIAN V. and POLLAK M., *Phys. Rev. B*, **47** (1993) 2038.
- [28] GASPARIAN V., ORTUÑO M., RUIZ J., CUEVAS E. and POLLAK M., *Phys. Rev. B*, **51** (1995) 6743.
- [29] GASPARIAN V., CHRISTEN T. and BÜTTIKER M., *Phys. Rev. A*, **54** (1996) 4022.
- [30] WIGNER E. P., *Phys. Rev.*, **98** (1955) 145.
- [31] SMITH F. T., *Phys. Rev.*, **118** (1960) 349.
- [32] GOLDBERGER M. and WATSON K., *Collision Theory* Dover books on physics (Dover Publications) 2004.
- [33] LOFY J., GASPARIAN V., GEVORKIAN Z. and JÓDAR E., *Reviews on Advanced Materials Science*, **59** (2020) 243.
- [34] GASPARIAN V., ORTUÑO M., RUIZ J. and CUEVAS E., *Phys. Rev. Lett.*, **75** (1995) 2312.
- [35] BENDER C. M., DUNNE G. V. and MEISINGER P. N., *Physics Letters A*, **252** (1999) 272.
- [36] SHIN K. C., *Journal of Physics A Mathematical General*, **37** (2004) 8287.
- [37] MUSSLIMANI Z. H., MAKRIS K. G., EL-GANAINY R. and CHRISTODOULIDES D. N., *Phys. Rev. Lett.*, **100** (2008) 030402.
- [38] MIDYA B., ROY B. and ROYCHOWDHURY R., *Physics Letters A*, **374** (2010) 2605.
- [39] GASPARIAN V., GUMMICH U., JÓDAR E., RUIZ J. and ORTUÑO M., *Physica B Condensed Matter*, **233** (1997) 72.
- [40] KORRINGA J., *Physica*, **13** (1947) 392.
- [41] KOHN W. and ROSTOKER N., *Phys. Rev.*, **94** (1954) 1111.
- [42] LÜSCHER M., *Nucl. Phys. B*, **354** (1991) 531.
- [43] BUSCH T., ENGLERT B.-G., RZAŻEWSKI K. and WILKENS M., *Found. Phys.*, **28** (1998) 549–559.
- [44] GUO P. and LONG B., *Journal of Physics G: Nuclear and Particle Physics*, **49** (2022) 055104.
- [45] GUO P. and GASPARIAN V., *Phys. Rev. D*, **103** (2021) 094520.
- [46] GUO P. and GASPARIAN V., *Journal of Physics A: Mathematical and Theoretical*, **55** (2022) 265201.
- [47] GUO P., *Phys. Rev. C*, **103** (2021) 064611.
- [48] GUO P. and GASPARIAN V., *arXiv preprint arXiv:2307.12951*, (2023) .
- [49] MOSTAFAZADEH A., *Phys. Rev. Lett.*, **102** (2009) 220402.
- [50] AHMED Z., *Journal of Physics A: Mathematical and Theoretical*, **42** (2009) 472005.
- [51] LONGHI S., *Phys. Rev. B*, **80** (2009) 165125.